Current cross correlators in mesoscopic conductors

Samuelsson, Martin Peter; Buttiker, Markus

Journal of Low Temperature Physics, Vol. 146, Nos. 1/2, January 2007 (© 2006)
DOI: 10.1007/s10909-006-9266-9

Current Cross Correlators in Mesoscopic Conductors

Peter Samuelsson[1] and Markus Büttiker[2]

[1] *Division of Mathematical Physics, Lund University, Sölvegatan 14 A, 223 62 Lund, Sweden*
E-mail: Peter.Samuelsson@teorfys.lu.se
[2] *Département de Physique Théorique, Université de Genève, 1211 Genève 4, Switzerland*

We present an investigation of current cross correlators in mesoscopic conductors. Making an analogy to the optical Hanbury Brown Twiss experiment we discuss how quantum statistical effects and two-particle interference effects can be investigated with current cross correlations. We also discuss how current cross correlations can be used for detecting two-particle entanglement and to perform quantum state tomography, a complete reconstruction of the density matrix of the quantum state emitted from a mesoscopic conductor.

PACS Numbers: 73.23.-b; 05.40.-a; 72.70.+m; 74.40.+k.

1. INTRODUCTION

During the last one and a half decade, there has been an increasing interest in the noise, or current correlations, in mesoscopic conductors. A large number of mesoscopic systems have been considered, both theoretically and experimentally, and many properties of the noise have been investigated. This development has been reviewed in Ref. 1 and the most recent works were discussed in Ref. 2. An area of noise research which is of particular interest is current cross correlators, the correlation of currents at different contacts in a mesoscopic conductor. Current cross correlations contain important information on the properties of mesoscopic conductors which in many situations is not available from autocorrelations or average current.

A lot of inspiration and motivation for current cross correlation investigations in mesoscopic conductors comes from the pioneering optical experiments by Hanbury Brown and Twiss.[3,4] Hanbury Brown and Twiss designed a new stellar interferometer based on light intensity cross correlations. The operation of their intensity interferometer was based on two fundamental and interrelated principles of quantum mechanics, (i) photons emitted from a thermal source show a tendency to bunch, a direct consequence of Bose-Einstein statistics and (ii) photons emerging from two uncorrelated sources gives rise to an interference pattern in intensity cross correlations but not in the intensities themselves, a consequence of the indistinguishablity of quantum particles.

In this paper, we will start by following the path of Hanbury Brown and Twiss but instead consider electrons in mesoscopic conductors. We will first discuss the scattering theory for current cross correlations[5] and the negative cross correlations in mesoscopic conductors arising as a consequence of the Fermionic statistics of the electrons. The experimental demonstrations[6,7] of negative cross correlations, performed in electronic beam splitters, will be discussed. Then we will continue with the proposals how to obtain positive cross correlations[8] and discuss the recent experiment[9] providing the first example of positive cross correlations in mesoscopic conductors.

Thereafter we turn to the second aspect of the Hanbury Brown and Twiss experiment, the intensity–intensity, or two particle, interference. We discuss in some detail the recent proposal[10] for a fermionic two-particle interferometer in a mesoscopic conductor. Interestingly, as was shown in Ref. 10, in the fermionic, in contrast to the bosonic, Hanbury Brown and Twiss experiment the two interfering particles can be entangled. This provides a link from Hanbury Brown and Twiss to the topic of entanglement in mesoscopic conductors, recently receiving a lot of interest. We discuss how current cross correlations can be used to detect entanglement of spatially separated particles. In particular, we show how a Bell inequality can be formulated in terms of current cross correlators.

The possibility to detect entanglement with current cross correlations leads up to the more general question: using current cross correlations, what is the maximum possible information one can obtain about a two-particle state emitted from a mesoscopic conductor. As was shown in Ref. 11, it is actually possible to reconstruct the entire two-particle density matrix from current cross correlations. Here we discuss this reconstruction, called quantum state tomography, in some detail and use the fermionic Hanbury Brown and Twiss setup as an example.

We emphasize that the focus of the paper will be on our own contributions to the field and we thus make no attempt to present a review on the subject.

2. SCATTERING THEORY

Scattering theory provides a qualitative as well as quantitative understanding of transport properties of mesoscopic conductors. A scattering theory for current correlations was presented by Büttiker,[5] Let us consider a general mesoscopic noninteracting scatterer connected to N ideal electronic reservoirs (a zero impedance environment) via single mode contacts, shown in Fig. 1. We first note that the average current I_α flowing into a reservoir α is given by Büttiker[12]

$$I_\alpha = \frac{e}{h} \int dE \sum_\beta |s_{\alpha\beta}|^2 (f_\beta - f_\alpha), \tag{1}$$

where $s_{\alpha\beta} = s_{\alpha\beta}(E)$ is the amplitude for a particle at energy E to scatter from terminal β to terminal α and $f_\alpha = f_\alpha(E, V_\alpha)$ is the Fermi-Dirac distribution function for reservoir α kept at a potential eV_α .

The low-frequency cross correlator $S_{\alpha\beta}$ of currents flowing into terminal α and β is defined as $(\alpha \neq \beta)$

$$S_{\alpha\beta} = \int dt \langle \Delta I_\alpha(t) \Delta I_\beta(0) + \Delta I_\beta(0) \Delta I_\alpha(t) \rangle, \tag{2}$$

where $\Delta I_\alpha(t)$ is the fluctuation of the current flowing in lead α, as $\Delta I_\alpha(t) = I_\alpha(t) - I_\alpha$. The current correlator can be expressed as[5]

$$S_{\alpha\beta} = -\frac{e^2}{h} \int dE \sum_{\gamma,\delta} s_{\alpha\gamma} s^*_{\beta\gamma} s^*_{\alpha\delta} s_{\beta\delta} f_\gamma f_\delta. \tag{3}$$

Importantly, as shown in Ref. 5, the cross correlations are manifestly negative, independent on the specific form of the scattering amplitudes, the applied voltages V_α or the temperature of the system. We note

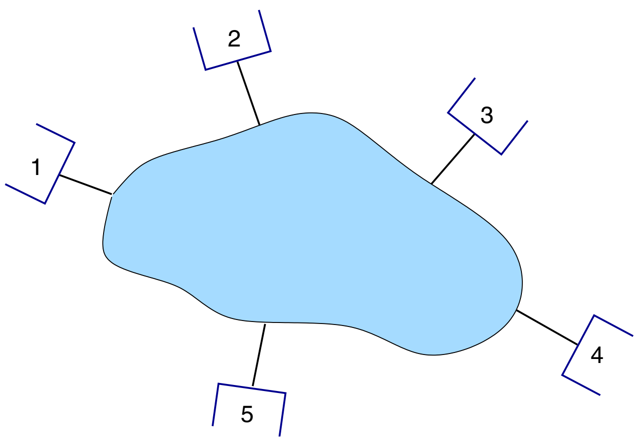

Fig. 1. (Color on-line). Mesoscopic conductor connected to $N = 5$ electronic reservoirs.

that for a thermal source of bosons, the same formula would hold but with opposite sign and Bose–Einstein distribution functions. The formulas above contain all the information needed for the investigations below.

3. HANBURY BROWN AND TWISS EXPERIMENT

In the mid-1950s Hanbury Brown and Twiss invented a new type of stellar interferometer, a tool to measure the angular diameter of stars.[3,4] The Hanbury Brown and Twiss (HBT) interferometer was the first example of an optical intensity interferometer. In an intensity, or two particle, interferometer the interference pattern is only present in the correlations between light intensities measured at two spatially separated detectors, and not in the intensities themselves. The HBT interferometer was thus different from the standard single particle Michelson interferometer where the interference pattern appeared directly in the intensity. The HBT intensity interferometer proved to be less sensitive to atmospheric scintillations compared to the Michelson interferometer, which allowed for a more accurate determination of the angular diameter. A schematic of the experimental setup as well as of the equivalent table top experiment are shown in Fig. 2.

The pioneering experiment of HBT demonstrated two important basic quantum mechanical principles. (i) Photons emitted from a thermal source show a tendency to bunch. This is a direct consequence of the Bose–Einstein distribution of the photons in the star. (ii) Photons emitted from two uncorrelated sources can give rise to a two-particle interference pattern in an intensity cross correlation experiment. This is a direct result of indistinguishability of identical quantum particles. The two-particle scattering process $1 \to A$ and $2 \to B$ can not be distinguished from the process $2 \to A$ and $1 \to B$ and consequently their amplitudes have to be added before calculating the probability of jointly detecting one particle in A and one in B.

It was clear[13] already at the time of HBT that a similar experiment could in principle be performed for electrons, however electrons emitted from a source in thermal equilibrium would instead show a tendency to anti-bunch, a consequence of the Fermi–Dirac distribution of the electrons in the source. It however turned out to be experimentally very difficult to perform an anti-bunching experiment with free fermions. This was due to the low occupation f of existing fermionic sources, which results in a very small cross correlation signal $\propto f^2$, as is clear from Eq. (2). Anti-bunching of free electrons was thus only reported a few years ago.[14] Fermionic anti-

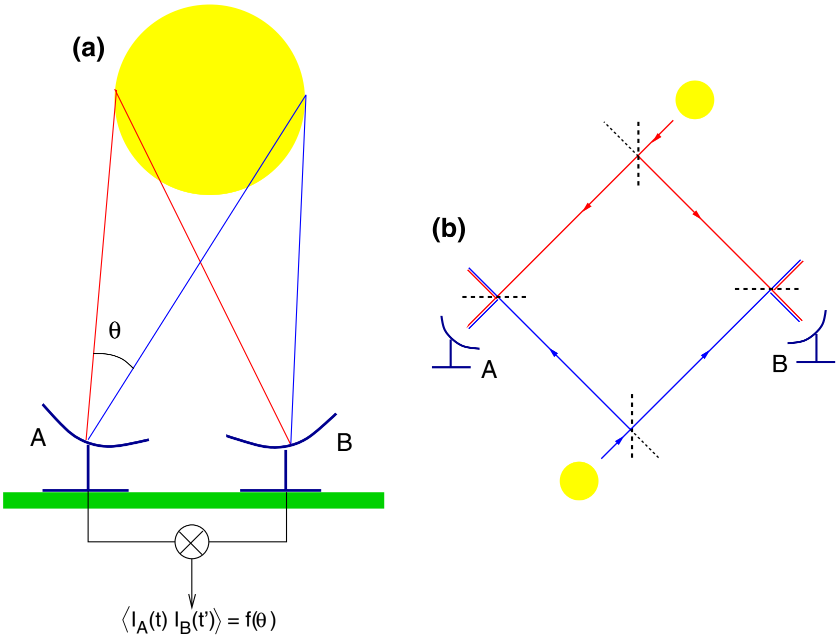

Fig. 2. (Color on-line). Left figure: schematic HBT setup, the angular diameter θ of a star is measured via cross correlations of the intensities at detectors at A and B. Right figure: equivalent table top HBT setup, the light from two independent sources are detected in A and B.

bunching was instead first demonstrated in mesoscopic conductors, where sources of electrons with essentially unity occupation was available in the form of electronic reservoirs at sub-Kelvin temperatures.

4. ELECTRONIC ANTIBUNCHING

In mesoscopic physics the main interest in the HBT experiment has until very recently concerned the aspect of electronic anti-bunching. The theory of Ref. 5, our Eq. (2), predicted negative cross correlations in mesoscopic conductors. The simplest possible system for investigating cross correlations is a reflectionless electronic beam splitter with transparency $T = 1 - R$, shown in Fig. 3. From Eq. (2) we get the simple formula for the cross correlations at zero temperature

$$S_{AB} = -\frac{2e^2}{h}|V|RT, \tag{4}$$

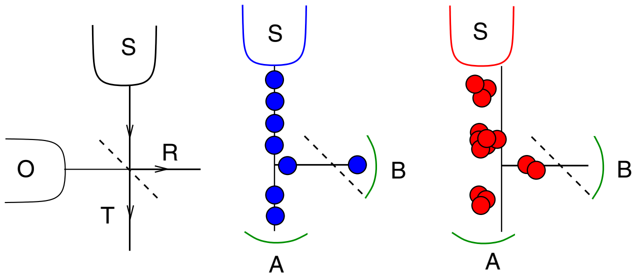

Fig. 3. (Color on-line). Left figure: electronic beam splitter with transparency $T = 1 - R$. Center figure: perfect anti-bunching of electrons emitted from an electron reservoir at zero temperature. Right figure: Bunching of photons emitted from a thermal source. In center and right figure, the cross correlations between currents or intensities in the detectors A and B are negative and positive, respectively.

where V is the voltage applied at the source S, keeping terminals A and B as well as the inactive injection terminal 0 at ground. The first demonstration of anti-bunching of electrons was provided in two independent experiments with electronic beam splitters, by Henny *et al.*[6] and Oliver *et al.*[7] The two experiments were however carried out under very different physical conditions. In Henny *et al.* experiment a conductor in strong magnetic field, in the quantum Hall regime was used where the transport takes place along edge states. In contrast, in Oliver *et al.* experiment a conductor at low magnetic field was used. Nevertheless, in both experiments the results were in very good agreement with the theoretical predictions. We also note that Oberholzer *et al.*[15] performed an additional experiment with a noisy incoming stream, to demonstrate explicitly that the negative cross correlations were not a consequence of a current conservation only.

5. POSITIVE CROSS CORRELATIONS

The result[5] that current cross correlations in normal state, noninteracting mesoscopic conductors are manifestly negative inspired a considerable amount of theoretical work on how to reverse the sign of the cross correlators. Interactions between the electrons as well as connecting the conductor to superconducting and ferromagnetic terminals were proposed, here we just refer the reader to recent reviews where these proposals are discussed.[2,16] We will instead focus on the theoretical proposal by Texier and Büttiker,[8] recently realized experimentally by Oberholzer *et al.*[9] In this experiment positive current correlations were observed for the first time in mesoscopic systems.

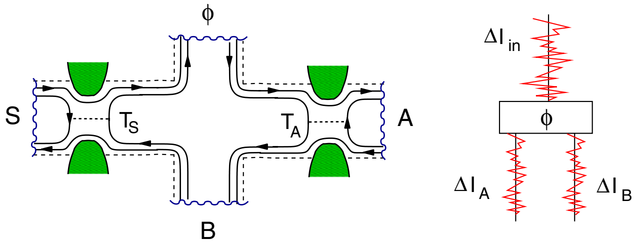

Fig. 4. (Color on-line). Left: a schematic of the quantum Hall geometry with two propagating edge states and two quantum point contacts acting as beam splitters. A voltage probe ϕ connected to the conductor gives rise to positive correlations between currents flowing into terminal A and B. Right: the role of the voltage probe as a noise divider.

A sketch of the system is shown in Fig. 4, a conductor in the quantum Hall regime with two propagating edge states. The edge states are quantum mechanical analogous of classical skipping orbits, with unidirectional transport of the electrons (the direction is denoted with arrows in the figure). Two quantum point contacts (QPC's) with tunable transparency act as electronic beam splitters for the inner edge state. The transparencies are T_S and T_A, respectively. The outer edge propagate without scattering (unity transparency) through the quantum point contacts.

The conductor is connected to three electronic reservoirs S, A and B with applied voltages $V_S = V$ and $V_A = V_B = 0$. Scattering at the QPC connected to the source reservoirs S introduces noise. The terminals A and B are used as detectors for the fluctuations. Moreover, a voltage probe ϕ, i.e., a terminal with the potential left floating, is also connected to the conductor. The voltage probe draws no current, its potential is oscillating in response to the injected charge, giving zero current (at low frequencies) into the probe. Following the theory of Texier and Buttiker, for a completely reflected inner edge state at A (corresponding to $T_A = 0$), the cross correlations between currents flowing into contacts A and B is, at zero temperature, given by

$$S_{AB} = \frac{e^2}{2h}|V|T_S(1 - T_S). \tag{5}$$

This is positive and just 1/4 of the magnitude of the fluctuation of the currents emitted from the first quantum point contact. This result can be understood in a very simple way. Since no current is drawn from the voltage probe, both the average current and the current fluctuations are conserved. The effect of the voltage probe is then simply to redistribute the incoming current, both average current and fluctuations, on the two outgoing egdechannels, as shown in Fig. 4. The voltage probe thus works as a noise divider and we can write $\Delta I_A = \Delta I_B = \Delta I_{\text{in}}/2$, where ΔI_{in} is the noise of the current flowing into the probe, created by the first point contact. This gives

$$\langle \Delta I_A \Delta I_B \rangle = \langle \Delta I_A^2 \rangle = \langle \Delta I_B^2 \rangle = \langle \Delta I_{\text{in}}^2 \rangle / 4. \tag{6}$$

In the experiment, a very good agreement with the theoretical predictions in Eq. (5) was found. In particular, by pinching off the contact between the voltage probe and the conductor, it was demonstrated that the positive correlations disappear. The system without the voltage probe is then just identical to the system studied in Ref. 15. We also point out that zero-magnetic field geometries with positive correlations generated by voltage probes have recently been discussed in Ref. 17. Very recently, positive correlations was also demonstrated in two additional experiments.[18,19]

6. TWO PARTICLE INTERFERENCE

We now turn to the second aspect of the HBT experiment, the interference between two particles originating from two different, uncorrelated sources. This two-particle interference is, as demonstrated by HBT, only present in the current, or intensity, cross correlations and not in the currents or intensities themselves. Recently, we proposed an experiment where this two-particle interference could be measured via the current cross correlations in a conductor in the quantum Hall regime.[10] A schematic of the setup is shown in Fig. 5.

The conductor is contacted to eight electronic reservoirs $\alpha = 1$ to 8 and four quantum point contacts $i = A, B, C$, and D. The reservoirs 2 and 3 are kept at a potential eV while the rest are grounded. The transport takes place along a single edge state, where the electrons pick up phases ϕ_1 to ϕ_4. An Aharonov–Bohm flux Φ penetrates the center of the sample. Importantly, the geometry has no interfering orbits. It is assumed that all edge states have the same length. Electron waves incident at the ith QPC are transmitted with amplitude $\sqrt{T_i}$ and reflected with amplitude $\sqrt{R_i}$ with $T_i + R_i = 1$.

The overall scattering amplitudes have a very simple form. A particle leaving source contact 2 can after transmission through QPC C reach either contact 5 or 6. For instance, the amplitude to scatter from 2 to 5 is $s_{52} = \sqrt{T_A}\exp(i\phi_1)\sqrt{T_C}$. Such a process is shown in Fig. 5. The current flowing into lead $\alpha = 5$ to 8 is given by Eq. (1)

$$I_\alpha = -(e/h)\int dE \left(|s_{\alpha 2}|^2 + |s_{\alpha 3}|^2\right)(f - f_0), \tag{7}$$

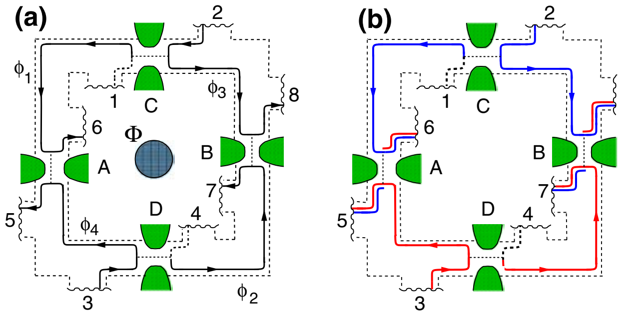

Fig. 5. (Color on-line). Left: two-source, four detector electrical Hanbury Brown and Twiss geometry: a conductor in the quantum Hall regime with eight terminals and four QPS's. Terminals 2 and 3 are sources of electrons (a voltage eV is applied against all other terminals). Electrons follow edge states in the direction indicated by the arrows and pick up phases ϕ_1 to ϕ_4. An Aharanov–Bohm flux Φ penetrates the center of the sample. Right: the paths from the sources to the detectors highlighted. Note that no paths form closed orbits.

where f is the Fermi distribution function of reservoirs 2 and 3 and f_0 the distribution function of the other reservoirs. Since the current depends only on the scattering probabilities $|s_{\alpha\gamma}|^2$, it follows immediately that in the set-up of Fig. 2 all currents are phase-insensitive, determined only by products of transmission and reflection probabilities of the QPC's.

For the current cross correlators, the situation is different. From Eq. (2) we get

$$S_{\alpha\beta} = -(2e^2/h)\int dE|s^*_{\alpha 2}s_{\beta 2} + s^*_{\alpha 3}s_{\beta 3}|^2(f - f_0)^2 \tag{8}$$

for $\alpha \neq \beta = 5$ to 8. For the simple case with transmission and reflection probabilities of all QPC's equal to 1/2, the correlation function of the currents at, e.g., contacts, 5 and 8 is then, at zero temperature

$$S_{58} = -(e^2/4h)|eV|[1 + \cos(\phi_1 + \phi_2 - \phi_3 - \phi_4)]. \tag{9}$$

The total phase $\phi_1 + \phi_2 - \phi_3 - \phi_4$ is just the phase of a single closed loop around the center of the system. Within our assumptions, the total phase depends only on the enclosed Aharonov–Bohm flux as $\phi_1 + \phi_2 - \phi_3 - \phi_4 = 2\pi\Phi/\Phi_0$, where $\Phi_0 = h/e$ is the flux quantum. The flux dependence of the current cross correlator

$$S_{58} = -(e^2/4h)|eV|[1 + \cos(2\pi\Phi/\Phi_0)], \tag{10}$$

together with a flux independent current I_α is thus an unambiguous signature of a two-particle Aharonov–Bohm effect.

To compare the electrical and the optical HBT effect it is interesting to consider in more detail the probability to jointly detect one particle at $\alpha = 5, 6$ and one at $\beta = 7, 8$. In optics, where photo-detectors are used to detect the particles, the joint probability of detecting two photons is given by the theory of Glauber.[20] In close analogy we defined in Ref. 10 the probability $P_{\alpha\beta}(\tau)$ of detection (at energy $0 < E < eV$) of one electron in detector α at time t and one in β at time $t + \tau$. For times τ much shorter than the typical time $\tau_C = h/eV$ between two electrons emitted from a reservoir one has a true coincidence measurement.

Although the joint detection probability can hardly be measured directly in a mesoscopic setup (in contrast to optics), it is still a conceptually relevant property, as is clear from the discussions below. Following Ref. 10 we get the joint detection probability for electrons (−) and photons (+)

$$\begin{aligned} P_{\alpha\beta}(\tau) \propto\ & |s_{2\alpha}|^2 |s_{2\beta}|^2 [1 \pm g(\tau)] + |s_{3\alpha}|^2 |s_{3\beta}|^2 [1 \pm g(\tau)] \\ & + |s_{2\alpha}|^2 |s_{3\beta}|^2 + |s_{3\alpha}|^2 |s_{2\beta}|^2 \\ & \pm g(\tau) \left[s_{2\alpha}^* s_{3\beta}^* s_{2\beta} s_{3\alpha} + s_{2\alpha} s_{3\beta} s_{2\beta}^* s_{3\alpha}^* \right], \end{aligned} \tag{11}$$

where $g(\tau) = \sin^2(\tau/\pi\tau_C)/(\tau/\pi\tau_C)^2$ contains the time dependence. For electrons $\tau_C = h/eV$ and for photons $\tau_C = 2/\pi\Delta$, with Δ the width in frequency of the light beam.

Several interesting conclusions can be drawn directly from Eq. (11). For $\tau \gg \tau_C$, $g(\tau)$ approaches zero and $P_{\alpha\beta}$ is just proportional to the product of the two mean currents/intensities. The fermionic versus bosonic statistics of the particle thus plays no role. For shorter times, $\tau \leqslant \tau_C$, $g(\tau)$ is finite and the statistics is important. As pointed out above, the statistics of the particles enter in two different ways. (i) The first two terms in Eq. (11) describe a direct bunching (+) or anti-bunching (−) effect for two particles emitted from the same reservoir within a time $\tau \leqslant \tau_C$. This effect would still be present if one of the source 2 or 3 is removed. (ii) The last two terms describe an exchange interaction, where the $\pm$ sign explicitly follows from the interchange of the two detected particles. This two-particle exchange interference[5] is only present when both sources are active.

Interestingly, we can directly relate the joint detection probability in Eq. (11) at times $\tau \ll \tau_C$ with the currents in Eq. (7) and the zero frequency noise correlators in Eq. (8) as $[g(0) = 1]$

$$\begin{aligned} P_{\alpha\beta}(0) & \propto \pm |s_{2\alpha} s_{2\beta}^* + s_{2\alpha} s_{2\beta}^*|^2 + \left(|s_{2\alpha}|^2 + |s_{3\alpha}|^2 \right) \left(|s_{2\beta}|^2 + |s_{3\beta}|^2 \right) \\ & \propto S_{\alpha\beta} + 2\tau_C I_\alpha I_\beta. \end{aligned} \tag{12}$$

The cross correlators $S_{\alpha\beta}$ for electrons and photons thus have opposite signs, as pointed out above. We note that similar short time correlators have been considered in mesoscopic conductors in, Refs. 21 and 22.

7. ENTANGLEMENT AND BELL INEQUALITIES

As was shown in Ref. 10, the two particle interference in the electronic HBT experiment is closely related to another intriguing property of quantum mechanics, namely entanglement. Entanglement was introduced as a concept in physics in the mid-1930s and was initially discussed in the context of fundamental properties of quantum mechanics. More recently it has been realized that entanglement constitutes a resource for quantum information and quantum computation.[23] The prospect of quantum information in solid state devices thus makes an investigation of entanglement in mesoscopic conductors of large interest.

Two particles are entangled if the total wavefunction of the particles can not be written as a product of the wavefunctions of the individual particles. A typical example is the spin singlet state $1/\sqrt{2}[|\uparrow\downarrow\rangle - |\downarrow\uparrow\rangle]$. Two entangled particles thus show a stronger nonlocal correlation than what is possible for non-entangled particles. A large number of works have been devoted to how to create entanglement in mesoscopic conductors, we do not discuss these different proposals here but only refer to a number of recent reviews on the subject.[24–26]

A standard way to test whether a pair of particles are entangled is to perform a Bell inequality test.[27] A Bell inequality is typically formulated in terms of joint probabilities to detect spatially separated particles. A schematic picture of a Bell setup for two spin 1/2 particles is shown in Fig. 6. A standard form of the Bell inequality[28] is expressed as

$$-2 \leq S_B \leq 2, \tag{13}$$

where S_B, the Bell parameter, is given by

$$S_B \equiv E(\phi_A, \phi_B) - E(\phi_A, \phi'_B) + E(\phi'_A, \phi_B) + E(\phi'_A, \phi'_B). \tag{14}$$

Here the function E is expressed in terms of the joint detection probabilities $P_{\alpha\beta}(\phi_A, \phi_B)$ to detect the particles in channel $\alpha = +, -$ at A at channel $\beta = +, -$ at B, as

$$E(\phi_A, \phi_B) = P_{++}(\phi_A, \phi_B) - P_{+-}(\phi_A, \phi_B) - P_{-+}(\phi_A, \phi_B) + P_{--}(\phi_A, \phi_B). \tag{15}$$

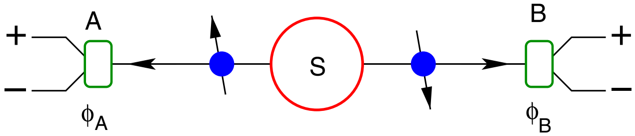

Fig. 6. (Color on-line). Schematic of Bell setup for entangled spin pairs. From the source S, a pair of entangled spins is emitted, with one particle propagating towards A and one toward B. At A and B, the spins are rotated an angle ϕ_A and ϕ_B (in the plane), respectively. The particles are then detected in electronic reservoirs $+$ and $-$.

For simplicity only inplane spin-rotations are considered, described by the scattering matrix at A

$$S_A = \begin{pmatrix} \cos(\phi_A) & -\sin(\phi_A) \\ \sin(\phi_A) & \cos(\phi_A) \end{pmatrix} \tag{16}$$

and similiarily at B. Several authors [10,21,22,29,30] have proposed to formulate a Bell Inequality in terms of current cross correlators. In our work[10] we showed that the current cross correlators in a system in the tunneling limit is directly proportional to the joint detection probabilities appearing in the Bell Inequality,

$$P_{\alpha\beta}(\phi_A, \phi_B) \propto S_{\alpha\beta}. \tag{17}$$

This allowed us to directly formulate a Bell Inequality in terms of low frequency current cross correlators. For the electronic HBT interferometer, the joint detection probabilities in Eq. (12) also contain information about the average currents. We showed in Ref. 10 that it is nevertheless possible to violate a Bell inequality, even if one does not work in the tunneling limit. Interestingly, this is not possible for the photonic HBT setup, due to the possibility of having two particles emitted simultaneously from a thermal photon source.

In our proposals, Refs. 29 and 10, we considered instead of spin entanglement a system with entanglement in the orbital degree of freedom. A typical orbital two-level system is a conductor with two transport modes. If the particle is in one mode, the system is in a pseudo-spin state $|\uparrow\rangle$ and if the particle is in the other mode it is in a pseudo-spin state $|\downarrow\rangle$. A schematic of a Bell setup for orbital entanglement is shown in Fig. 7.

The main advantage of orbital entanglement compared to spin entanglement is that the orbital entanglement can be manipulated with standard electronic beam splitters and directly detected via current cross correlations. In the case with spin entanglement one needs first to convert the spin information to charge or orbital information before the state can be detected.

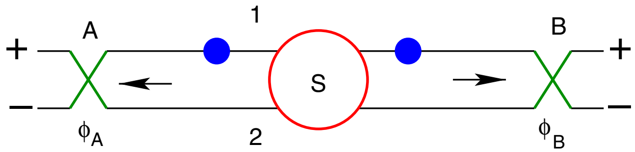

Fig. 7. (Color on-line). Schematic of Bell setup for pairs of orbitally entangled electrons. From the source S, a pair of entangled particles is emitted, with one particle propagating towards A and one toward B. At A and B, the orbital states are rotated via electronic beam splitters an angle ϕ_A and ϕ_B, respectively. The particles are then detected in electronic reservoirs $+$ and $-$.

8. QUANTUM STATE TOMOGRAPHY

A Bell inequality works as a witness of entanglement, if the inequality is violated the state is entangled. We note however that the opposite is not true, there exist entangled states[31] that do not violate a Bell inequality. Moreover, the degree of violation of a Bell Inequality can typically not be used as a measure of the entanglement. This raises the question if there is some other way to completely characterize the entanglement of a quantum state emitted from a mesoscopic conductor.

The most general description of a two-particle state emitted from a mesoscopic conductor is given in terms of the two-particle density matrix ρ. The density matrix ρ by definition determines any two-particle observables on the state.[32] Moreover, the entanglement of the state is determined by the two-particle density matrix. It is therefore natural to try to investigate to what extent the density matrix can be characterized by current cross correlations, the typical two-particle observable in mesoscopic systems.

Very recently we showed that it is indeed possible to reconstruct the entire density matrix via shot noise correlations.[11] Such a reconstruction procedure is known as quantum state tomography and has been proposed theoretically and performed experimentally on several different quantum systems. In particular, in close analogy to our system, it has been performed experimentally on entangled two-photon states.[33–35] In our proposal we considered a mesoscopic conductor, coupled to four leads $A1$,$A2$,$B1$, and $B2$ (see Fig. 8). The mesoscopic conductor acts as a source of orbital quantum states. The leads form local orbital two-level systems, with basis states $|1\rangle$ and $|2\rangle$, respectively. The emitted state to be characterized is manipulated and detected in regions A and B, containing experimentally realizable beam splitters and phase gates. The combined beam splitter-phase gate structure can generally be characterized by a scattering matrix (at A)

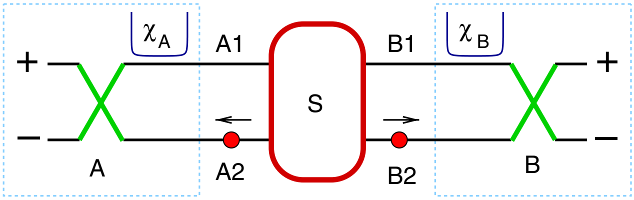

Fig. 8. (Color on-line). A mesoscopic conductor acting as a source (S) for quantum states, is connected to four leads $A1$, $A2$, $B1$, and $B2$. The leads are further connected to two regions (dashed boxes) A and B where the state is manipulated and detected. The regions contain beamsplitters (crosses) and phase gates (open boxes).

$$S_A = \begin{pmatrix} \sqrt{R_A}e^{i\varphi_{A2}} & \sqrt{T_A}e^{i(\varphi_{A3}-\chi_A)} \\ \sqrt{T_A}e^{i(\varphi_{A1}+\varphi_{A2})} & -\sqrt{R_A}e^{i(\varphi_{A1}+\varphi_{A3}-\chi_A)} \end{pmatrix} \tag{18}$$

with arbitrary phases φ_{Ak}, $k=1$ to 3, and an adjustable gate phase χ_A. Phase gates were, e.g., recently demonstrated experimentally in interferometers in quantum Hall systems,[36,37] by modulating the length of the electron paths. The beam splitters are further connected to reservoirs + and −, where the currents are measured.

Introducing operators $b_{An}^{\dagger}$ creating electrons in lead An, with $n=1,2$, propagating out from the source, the one-particle density matrix is defined as

$$\rho_A = \sum_{n,m=1}^{2} \rho_{nm} b_{An}^{\dagger}|0\rangle\langle 0|b_{Am} = \begin{pmatrix} \rho_{11} & \rho_{12} \\ \rho_{21} & \rho_{22} \end{pmatrix}. \tag{19}$$

Here we work in the basis $\{|1\rangle_A, |2\rangle_A\}$, with $b_{An}^{\dagger}|0\rangle = |n\rangle_A$. The matrix elements $\rho_{nm} = \langle b_{Am}^{\dagger} b_{An}\rangle$. In the same way, the two-particle density matrix is given by

$$\rho_{AB} = \sum_{n,m,k,l=1}^{2} \rho_{nm}^{kl} b_{An}^{\dagger} b_{Bk}^{\dagger}|0\rangle\langle 0|b_{Bl}b_{Am}, \tag{20}$$

with the matrix elements $\rho_{nm}^{kl} = \langle b_{Am}^{\dagger} b_{Bl}^{\dagger} b_{Bk} b_{An}\rangle$. Here only the nonlocal density matrix, describing correlations between particles at A and B, is considered.

The one and two-particle density matrices of the emitted state can be parameterized as

$$\rho_A = \frac{1}{2}\sum_{i=0}^{3} c_i \sigma_i = \frac{1}{2}\begin{pmatrix} c_0 + c_3 & c_1 - ic_2 \\ c_1 + ic_2 & c_0 - c_3 \end{pmatrix} \tag{21}$$

and similarly at B and

$$\rho_{AB} = \frac{1}{4}\sum_{i,j=0}^{3} c_{ij}\sigma_i \otimes \sigma_j, \tag{22}$$

where the c-coefficients are real and σ_j are the Pauli matrices, with $j = 0, x, y$ and z and $\sigma_0 = 1$. In the linear voltage regime, for a single spin direction, the average current at terminal A+ can be written

$$I_A^+/(e^2V/h) = \mathrm{tr}\,(\rho_A \mathcal{A}) \tag{23}$$

with the matrix expressed in terms of the scattering amplitudes of beam splitter and phase gates

$$\mathcal{A} = \begin{pmatrix} R_A & \sqrt{T_A R_A} e^{-i(\chi_A + \varphi_A)} \\ \sqrt{T_A R_A} e^{i(\chi_A + \varphi_A)} & T_A \end{pmatrix} \tag{24}$$

with $\varphi_A = \varphi_{A2} - \varphi_{A3}$. The zero frequency current cross correlator together with the currents at $A+$ and $B+$ can be written in terms of the two-particle density matrix as

$$\frac{S_{AB}^{++}}{2e^3V/h} + \frac{I_A^+ I_B^+}{(e^2V/h)^2} = \mathrm{tr}\,(\rho_{AB}\mathcal{A} \otimes \mathcal{B}), \tag{25}$$

where $\mathcal{B}$ is given from in Eq. (24) by changing the index $A \to B$. Importantly, only four different settings of the scattering parameters at A and four at B are needed to completely reconstruct the two-particle density matrix. Moreover, only currents at contacts $A+$ and $B+$ need to be measured. By then performing a set of sixteen noise measurements and eight current measurements (four at A and four at B), it is possible to obtain all the sixteen coefficients parameterizing ρ_{AB}. For details of this derivation we refer to Ref. 11.

For the entanglement, it is interesting to compare the quantum state tomography approach to the Bell inequality approach. The same number of noise and current measurements are needed for the tomography as for the Bell Inequality. However, to completely reconstruct an unknown density matrix, one needs to work with phase gates, which introduces additional complexity when performing the experiment.

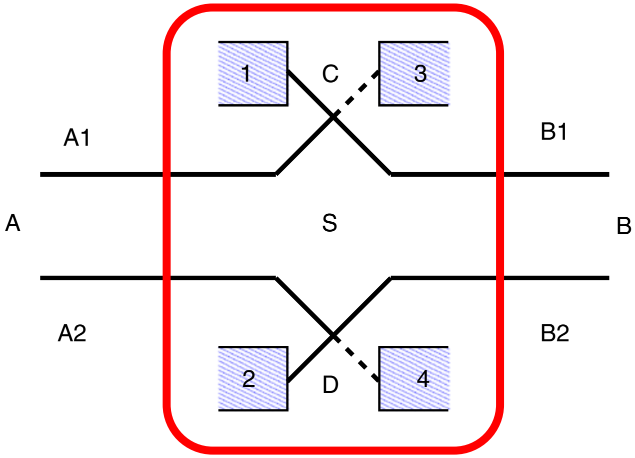

Fig. 9. (Color on-line). Schematic of the HBT geometry in a tomography setup. Two reservoirs biased at eV, 1 and 2, and two grounded reservoirs, 3 and 4, are connected via beam splitters to the four leads going out towards A and B. Scattering between upper and lower leads, e.g., $A1$ and $A2$, is not possible.

It is instructive to demonstrate the principle of quantum state tomography on a concrete example. We therefore consider the two-particle HBT geometry discussed above, shown in a tomography setup in Fig. 9 (note that the lead notation conforms with Ref. 11 but not with Fig. 5). We assume that the scattering at the point contacts C and D is described by scattering matrices

$$S_C = \begin{pmatrix} r_C & t_C \\ t'_C & r'_C \end{pmatrix}, \qquad S_D = \begin{pmatrix} r_D & t_D \\ t'_D & r'_D \end{pmatrix}. \tag{26}$$

The state incident on the two point contacts C and D is given by (at a single energy and spin direction)

$$|\Psi_{\text{in}}\rangle = |1\rangle|2\rangle, \tag{27}$$

where $1, 2$ denotes the reservoirs from which the particles emerge. The state going out from the point contacts C and D toward A and B is then given by, using the scattering matrices in Eq. (26),

$$|\Psi_{\text{out}}\rangle = r_C t_D |1\rangle_A |2\rangle_B - t_C r_D |2\rangle_A |1\rangle_B + t_C t_D |1\rangle_B |2\rangle_B + r_C r_D |1\rangle_A |2\rangle_A. \tag{28}$$

Here the index A, B denotes toward which region the particle is propagating. From the definition of the reduced single particle density matrix in

Eq. (21), one finds at A

$$\rho_A = \begin{pmatrix} R_C & 0 \\ 0 & R_D \end{pmatrix}, \tag{29}$$

working in the basis $\{|1\rangle_A, |2\rangle_A\}$, i.e., $(\rho_A)_{ij} = \langle \Psi_{\text{out}}|i\rangle\langle j|\Psi_{\text{out}}\rangle$ with $i, j = 1, 2$. The matrix at B is found in a similar way. The off-diagonal elements are zero since scattering between the upper and lower arms is impossible. The two-particle density matrix, defined in Eq. (22), is along the same lines given by

$$\rho_{AB} = \begin{pmatrix} 0 & 0 & 0 & 0 \\ 0 & |r_C t r_D|^2 & -r_C r_D^* t_C^* t_D & 0 \\ 0 & -r_C^* r_D t_C t_D^* & |t_C t_D|^2 & 0 \\ 0 & 0 & 0 & 0 \end{pmatrix}, \tag{30}$$

where we are working in the basis $\{|1\rangle_A|1\rangle_B, |1\rangle_A|2\rangle_B, |2\rangle_A|1\rangle_B, |2\rangle_A|2\rangle_B\}$. The reduced two-particle state is actually a pure state, $\rho_{AB} = |\Psi\rangle\langle\Psi|$ with

$$|\Psi\rangle = r_C t_D |1\rangle_A |2\rangle_B - t_C r_D |2\rangle_A |1\rangle_B. \tag{31}$$

This can be understood directly from Eq. (28) by realizing that the only part of the state that contributes to the reduced two-particle density matrix is the one which contains one particle at A and one at B. For identical beam splitters C and D the state $|\Psi\rangle\langle\Psi|$ is actually an orbital singlet. The density matrix ρ_{AB} can then be characterized by performing current and current correlation measurements, as discussed above. As shown in Ref. 11, for the HBT-geometry, the number of measurements needed to reconstruct the density matrix is less than sixteen, due to the topological properties of the geometry.

It is important to note that the superposition in Eq. (31) is a consequence of the indistinguishability of the two electrons. One electron is emitted from reservoir 1 and one from 2 and one electron is scattered towards A and one towards B. Since the two alternatives 1 to A and 2 to B and 1 to B and 2 to A are indistinguishable, the quantum state is a superposition of the two corresponding probability amplitudes. As was shown in Ref. 10, this exchange interference gives rise to two-particle interference, a two-particle Aharonov–Bohm effect detectable in the current noise. As is clear from above, it is also responsible for the entanglement of the state.

9. CONCLUSIONS

In conclusion, we have presented an investigation of current cross correlators in mesoscopic conductors. We first discussed the optical Hanbury

Brown and Twiss interferometer, where intensity cross correlations were used to investigate the angular diameter of stars. As an analogy to the Hanbury Brown and Twiss experiment we first discussed quantum statistical effects, bunching and anti-bunching, in mesoscopic conductors. Thereafter, we investigated two-particle interference in fermionic system, focusing on the setup proposed in Ref. 10. We also discussed how to formulate a Bell inequality in terms of current cross correlations and how this can be used to detect two-particle entanglement. Finally we presented a scheme for quantum state tomography, a complete reconstruction of the quantum state emitted by a mesoscopic conductor, using current cross correlations.

ACKNOWLEDGMENTS

This research was supported by the Swedish VR, the Swiss NSF and MANEP.

REFERENCES

1. Ya. M. Blanter and M. Büttiker, *Phys. Rep.* **336**, 1 (2000).
2. Ya. M. Blanter (unpublished), cond-mat/0511478.
3. R. Hanbury Brown and R. Q. Twiss, *Nature* **177**, 27 (1956).
4. R. Hanbury Brown and R. Q. Twiss, *Nature* **178**, 1046 (1956).
5. M. Büttiker, *Phys. Rev. B* **46**, 12485 (1992).
6. M. Henny, S. Oberholzer, C. Strunk, T. Heinzel, K. Ensslin, M. Holland, and C. Schönenberger, *Science* **284**, 296 (1999).
7. W. D. Oliver, J. Kim, R. C. Liu, and Y. Yamamoto, *Science* **284**, 299 (1999).
8. C. Texier and M. Büttiker, *Phys. Rev. B* **62**, 7454 (2000).
9. S. Oberholzer, E. Bieri, C. Schoenenberger, M. Giovannini, and J. Faist, *Phys. Rev. Lett.* **96**, 046804 (2006).
10. P. Samuelsson, E. V. Sukhorukov, and M. Büttiker, *Phys. Rev. Lett.* **91**, 157002 (2003).
11. P. Samuelsson, and M. Büttiker, *Phys. Rev. B* **73**, 041305 (2006).
12. M. Büttiker, *Phys. Rev. Lett.* **57**, 1761 (1986).
13. E. M. Purcell, *Nature* **178**, 1449 (1956).
14. H. Kiesel, A. Renz, and F. Hasselbach, *Nature* **418**, 392 (2002).
15. S. Oberholzer, M. Henny, C. Strunk, C. Schönenberger, T. Heinzel, K. Ensslin, and M. Holland, *Physica E* **6**, 314 (2000).
16. M. Büttiker, in *Quantum Noise*, Yu. V. Nazarov and Ya. M. Blanter (eds.), Kluwer, Dordrecht (2003).
17. V. S. Rychkov and M. Büttiker, *Phys. Rev. Lett.* **96**, 166806 (2006).
18. Y. Chen and R. A. Webb, *Phys. Rev. Lett.* **97**, 066604 (2006).
19. D. T. McClure, L. DiCarlo, Y. Zhang, H.-A. Engel, C. M. Marcus, M. P. Hanson, A. C. Gossard (unpublished), cond-mat/0607280.
20. R. J. Glauber, *Phys. Rev.* **130**, 2529 (1963).
21. N. M. Chtchelkatchev, G. Blatter, G. B. Lesovik, and T. Martin, *Phys. Rev. B* **66**, 161320 (2002).
22. A. V. Lebedev, G. B. Lesovik, and G. Blatter, *Phys. Rev. B* **71**, 045306 (2005).
23. M. Nielsen and I. Chuang, *Quantum Computation and Quantum Information*, Cambridge University Press, Cambridge (2000).

24. C. W. J. Beenakker, in *Quantum Computers, Algorithms, and Chaos, International School of Physics Enrico Fermi*, Vol. 162 (unpublished), cond-mat/0508488.
25. P. Recher, D. S. Saraga, and D. Loss, in *Fundamental Problems of Mesoscopic Physics Interaction and Decoherence*, I. V. Lerner *et al*. (eds.), NATO Science Ser. II, Vol. 154, Kluwer, Dordrecht (2004), pp. 179–202.
26. T. Martin, A. Crepieux, and N. Chtchelkatchev, in *Quantum Noise*, Yu. V. Nazarov and Ya. M. Blanter, (eds.), Kluwer, Dordrecht (2003).
27. J. S. Bell, *Physics* **1**, 195 (1965); *Rev. Mod. Phys.* **38**, 447 (1966).
28. J. F. Clauser, M. A. Horne, A. Shimony, and R. A. Holt, *Phys. Rev. Lett.* **23**, 880 (1969).
29. P. Samuelsson, E. V. Sukhorukov, and M. Büttiker, *Phys. Rev. Lett*. **92**, 026805 (2004).
30. C. W. J. Beenakker, C. Emary, M. Kindermann, and J. L. van Velsen, *Phys. Rev. Lett.* **91**, 147901 (2003).
31. R. F. Werner, *Phys. Rev. A* **40**, 4277, (1989).
32. U. Fano, *Rev. Mod. Phys.* 29, 74 (1957).
33. A. G. White, D. F. V. James, P. H. Eberhard, and P. G. Kwiat, *Phys. Rev. Lett.* **83**, 3103 (1999).
34. P. G. Kwiat, S. Barraza-Lopez, A. Stefanov, and N. Gisin, *Nature* **409**, 1014 (2001).
35. T. Yamamoto, M. Koashi, S. K. Özdemir, and N. Imoto, *Nature* **421**, 343 (2003).
36. Y. Ji, Y. Chung, D. Sprinzak, M. Heiblum, D. Mahalu, and H. Strikman, *Nature* **422**, 415 (2003).
37. L. V. Litvin, H.-P. Tranitz, W. Wegscheider, and C. Strunk (unpublished), cond-mat/0607758.